Preprints (www.preprints.org) | NOT PEER-REVIEWED | Posted: 17 May 2023 doi:10.20944/preprints202305.1250.v1

Disclaimer/Publisher's Note: The statements, opinions, and data contained in all publications are solely those of the individual author(s) and contributor(s) and not of MDPI and/or the editor(s). MDPI and/or the editor(s) disclaim responsibility for any injury to people or property resulting from any ideas, methods, instructions, or products referred to in the content.

Article

Synthesis and characterization of Nd:YAG ceramics for laser applications

Olga A. Echartea-Reyes[1], Gloria V. Vázquez-García[2], José A. Castillo-Robles[3], Juan López-Hernández[4], Carlos A. Calles-Arriaga[5], Wilian J. Pech-Rodríguez[6] and Enrique Rocha-Rangel[7]*

[1] Universidad Politécnica de Victoria; oechartear@upv.edu.mx
[2] Centro de Investigaciones en Óptica, Laboratorio de Óptica Integrada; gvvazquez@cio.mx
[3] Universidad Politécnica de Victoria; jcastillor@upv.edu.mx
[4] Universidad Politécnica de Victoria; jlopezh@upv.edu.mx
[5] Universidad Politécnica de Victoria; ccallesa@upv.edu.mx
[6] Universidad Politécnica de Victoria; wpechr@upv.edu.mx
[7] Universidad Politécnica de Victoria; erochar@upv.edu.mx
* Correspondence: erochar@upv.edu.mx; Tel.: (+52-834-171-1100)

Abstract: Materials known as Nd:YAG are crystalline materials of the cubic system made from neodymium-doped yttrium aluminum garnet, which among others, have excellent optical properties. Nd:YAG four-level laser devices are highly used in both the health and industrial sectors. In this study, a simple and inexpensive alternative to manufacturing Nd:YAG materials through solid state reactions following powder processing routes was proposed. For this, an intense mixture of the precursor materials (Al_2O_3 and Y_2O_3) was carried out, followed by the addition of neodymium atoms to improve the optical properties of the resulting material. High energy mechanical mixing of the precursor powders resulted in submicron particles, with good size distributions of the powders. The advance of YAG formation was monitored by intermediate phase formation during heat treatment through interrupted tests at different temperatures and analysis by X-ray diffraction. From this analysis, it was found that reaction for the formation of the desired YAG is completed at 1500°C. Fourier-transform infrared spectroscopy analyses determined the presence of functional groups corresponding to the YAG. Finally, the study by optical emission spectroscopy showed wavelengths in agreement with the electronic structure of the elements of the synthesized Nd:YAG.

Keywords: Nd-YAG; Laser; Optical characterization.

1. Introduction

Materials known as neodymium-doped yttrium aluminum garnet (Nd:YAG) are crystalline materials of the cubic system made from neodymium-doped yttrium aluminum garnet, which has excellent physical, chemical, thermal, mechanical, and optical properties [1-7]. One of the applications of this type of material is its widespread use in white light emitters manufacturing. However, the development of lasers has always been conditioned by the availability of suitable materials for their use. In 1995, Ikesue et al. demonstrated that transparent Nd:YAG ceramics could be produced using ceramic fabrication techniques such as dry pressing and sintering [2]. Therefore, sintering of active media by ceramic methods has become an alternative for solid-state laser active media manufacturing. Ceramic processing allows functional dopant gradients to aid thermal management, increase pumping efficiency and add functional elements such as Q-switches to the active medium [3].

There are different synthesis routes for Nd:YAG among which the solid-state reaction, the solvo-thermal synthesis and the sol-gel route stand out [4,5]. Liquid-phase sintered materials are generally deteriorated by prolongation of the final stage. In addition, the use of additives used in the sintering of transparent ceramics while contributing to the

© 2023 by the author(s). Distributed under a Creative Commons CC BY license.

Preprints (www.preprints.org) | NOT PEER-REVIEWED | Posted: 17 May 2023 doi:10.20944/preprints202305.1250.v1

process, have at the same time been identified as the cause of optical defects [6]; so the synthesis of YAG by means of solid-state reactions is therefore of interest, in addition to the simplicity and low cost of this process.

In optical applications, such as lasers, it is suggested that the materials to be worked with must have a series of characteristics such as being homogeneous, i.e., without the presence of second phases with different refractive index and isotropic; the main limitation of ceramic materials is related to the scattering of light due to residual porosity [8]. Chemical structures, compositions, and crystalline contents influence the transparency of ceramic materials. It has been shown that the transparency and therefore the laser efficiency are rapidly reduced and with the presence of pores [9]. This is the reason that has prompted the development of transparent optical materials focusing on materials with cubic structure.

Technological advances in the synthesis, shaping, and sintering of ceramic powders have made it possible to adapt the microstructural, mechanical, and optical property relationships in the case of this type of materials [10]. Emphasizing the optical properties, the general condition sought in improving them is their homogeneity with respect to their dielectric properties through solid-state sintering. In order to optimize the reactive solid-state sintering process, Vorona et al. studied the phase composition, microstructure and optical properties of YAG ceramics doped with 0 ÷ 0.15% by weight of MgO; after analyzing the characteristics of Mg^{2+} ions, they concluded that the optimal concentration range of MgO sintering contributes to achieving transparent YAG ceramics [11]. Along the same line of research, Wentao Jia studied the quantitative relationship between microstructure and mechanical and optical properties in transparent Nd:YAG ceramics. In his study, W. Jia applied stereology and fractals to identify the quantitative relationship between them and mechanical properties of transparent Nd:YAG ceramics sintered at 1750ºC for 8-50 h [12]. The improvement of laser performance in transparent Nd:YAG ceramics has been investigated by Yuelong Fu et al. with preparations of 2% Nd:YAG ceramics using a solid-state reactive sintering method [13]. The sintered samples were annealed at different temperatures for different times, obtaining ceramics with high density and homogeneous structure with an average grain size of 15 μm. They concluded that, at 1450 °C and 5 hours of retention, the concentration of color centers in the sample is relatively low and the efficiency of the laser slope is the highest.

In addition to the study of the different types of properties and the way they are linked to each other and how they end up affecting the performance of lasers due to their optical properties, there are authors who in their studies pay special attention to the behavior and nature of carbon contaminations, dispersed in the matrix of yttrium aluminum garnet. Kosyanov et al., showed that an increase in applied pressure from 30 to 70 MPa changed the color of the ceramic; the samples darkened and became dark brown, affecting the optical properties of the material [13, 14]. To the best of our knowledge, there is no genuine interest in developing improvements in the optical properties by starting from the solid-state sintering of powders and emphasizing the economic and methodological advantages that this type of treatment presents, so the work to be done is promising in this area. In addition, the grinding parameters are usually not as long as those previously mentioned, so that the grinding time represents another advantage for its realization.

2. Materials and Methods

For the present study, the $Y_3Al_5O_{12}$ perovskite was synthesized. For this purpose, a mixture in stoichiometric amounts according to the reaction 1 was prepared.

$$3Y_2O_3 + 5Al_2O_3 \longrightarrow 2Y_3Al_5O_{12} \quad (1)$$

Powders of Y_2O_3 and Al_2O_3 (Sigma-Aldrich, 99.9 % purity and 1 ◎m size) were ground in a planetary mill (Retsch PM 100, Germany) during 3 hours at a rotation speed of 300 rpm. Also, a stainless-steel container with zirconia grinding elements of 0.3 cm diameter

Preprints (www.preprints.org) | NOT PEER-REVIEWED | Posted: 17 May 2023 doi:10.20944/preprints202305.1250.v1

was utilized, as well as, a powder weight/ball weight ratio of 1:12. After milling, the particle size distribution and specific surface area were determined using a Mastersizer 2000 equipment of English origin. The powders' mixtures resulting from the milling step were subjected to a thermal treatment at 900, 1,100, 1,300, and 1,500 °C, in order to follow the advance of reaction 1. The thermal treatment was carried out in an electric resistance furnace (Carbolite RHF17/3E, England) for 1 hour, as well as the heating sped was 25 °C/min. The advance of the chemical reaction was followed by X-ray diffraction analysis (Siemens, D-5000, Germany). Once the formation temperature of the compound $Y_3Al_5O_{12}$ was determined (reaction 1 complete), mixtures were prepared with the two initial components with additions of neodymium (0, 0.25, 0.5 and 1 atomic %). These mixtures were carried out in the planetary mill; the powders were mixed under the same conditions mentioned at the beginning of this methodology. With the powders resulting from the second grinding stage, cylindrical tablets 1 cm in diameter by 0.3 cm thick were obtained by uniaxial compaction at 250MPa using a press (Porter-30T, Mexico), which were then subjected to sintering treatments for 2h at 1500°C in an electric furnace. The density of the sintered samples was evaluated through the Archimedean principle, using standards established in the ASTM C20-00 standard [15]. To determine the functional groups, present in the compound formed, FTIR analysis was performed (Rayleight WQF-510A, China). The pump source used to obtain the emission spectra, was a laser diode that operates at 806 nm with an optical power of 80 mW; the laser light was collimated by a microscope objective of 10X. The absorption spectra of the pills were measured using a Cary 5000 UV-Vis-NIR spectrophotometer, in which the sample was placed so that the waveguides were perpendicular to the incident light beam and a range of 300-900 nm so that it could cover the main absorption bands of the material. Finally, observations of microstructure of sintered samples were performed by optical microscopy (Nikon Eclipse Ma200, Japan).

3. Results

3.1. Density

Figure 1 shows the apparent density achieved by the sintered samples as a function of the Nd content. What is observed in this figure is that as the Nd content increases, the density of the samples tends to decrease, this is probably because the melting point of Nd is 1,024°C. If the samples were sintered at 1,500°C, the Nd at that temperature must have been in liquid phase and, due to its low wettability, could not move within the mixture to occupy the porosity of the mixture which caused the porosity was not closed during sintering.

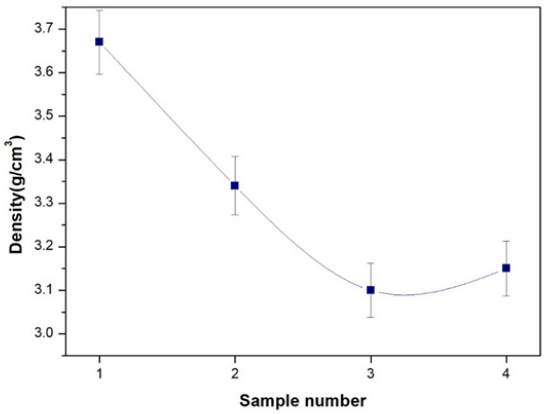

Figure 1. Apparent density of sintered $Y_3Al_5O_{12}$ as a function of the Nd content in it.

3.2 Particle size

Figure 2 shows the results of the particle size distribution analysis for each of the study samples. The figure shows that the particle sizes varied from less than 1 micron to several

Preprints (www.preprints.org) | NOT PEER-REVIEWED | Posted: 17 May 2023 doi:10.20944/preprints202305.1250.v1

microns; the sample with 0.5 at. % Nd exhibited the largest size distribution, with sizes ranging from 0.2 microns to 9 microns. On the other hand, the sample with 1 at. %Nd is the one with the smallest size distribution, since the particle sizes range between 0.2 and 2.5 microns. The sample with 0.25 at. % Nd also shows sizes below 1 micron and maximum sizes of approximately 5 microns. In comparison, the sample without Nd addition presents sizes between 2 and 5 microns. The strong size variation, especially due to the large particle sizes in the sample with 0.5%Nd, is what causes the densification in this sample to be not so good since during the compaction of the powders in this sample there must have been empty spaces (pores) difficult to close with sintering. According to these results, the samples without Nd and with low Nd content (0.25 % Nd) are the ones that densified better. Therefore, the size distribution of these samples is the one that favors the porosity closure during sintering. As mentioned before, the presence of Nd hinders the sintering of the compounds, due to the liquid state in which it is present at the temperature (1,500°C) of formation of the compound ($Y_3Al_5O_{12}$), which corresponds to the sintering temperature.

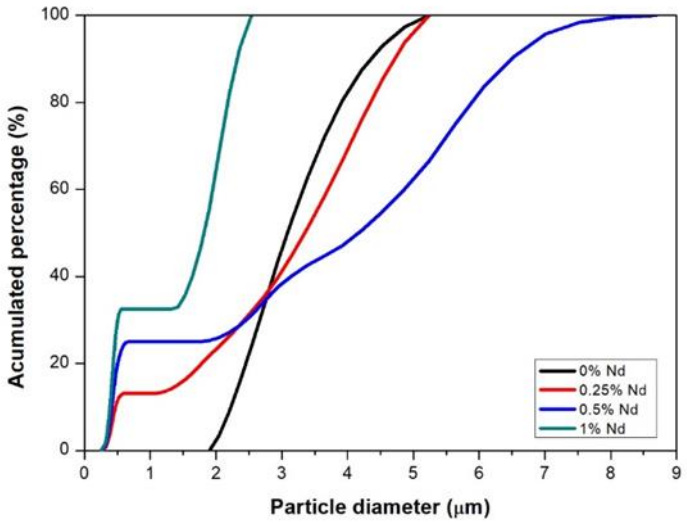

Figure 2. Particle size distribution of ground powders with different neodymium additions.

3.3 Crystalline structure

Figure 3 shows the diffraction patterns of the Y_2O_3 + Al_2O_3 powder mixture that was subjected to interrupted tests at different temperatures to observe the progress of reaction 1 and to determine the formation of the $Y_3Al_5O_{12}$ compound. In this figure, it can be seen that at 900°C reaction 1 has not started. This can be affirmed because the crystalline phases present here correspond to the 2 original components of the sample Y_2O_3 + Al_2O_3. At 1,100°C, the first traces of the desired garnet formation begin to appear, becoming more abundant at 1,300°C. At 1,500°C the predominant crystalline phase in the sample corresponds to that of yttrium aluminum garnet ($Y_3Al_5O_{12}$), although some traces of the alumina phase are still observed in the corresponding spectrum. The minimal width of the peaks and their intensity indicate the strong crystallinity of the compound formed. From these spectra, it can be summarized that reaction 1 starts to occur at approximately 1,100°C and is completed at 1,500°C, the latter being the formation temperature of $Y_3Al_5O_{12}$.

Preprints (www.preprints.org) | NOT PEER-REVIEWED | Posted: 17 May 2023 doi:10.20944/preprints202305.1250.v1

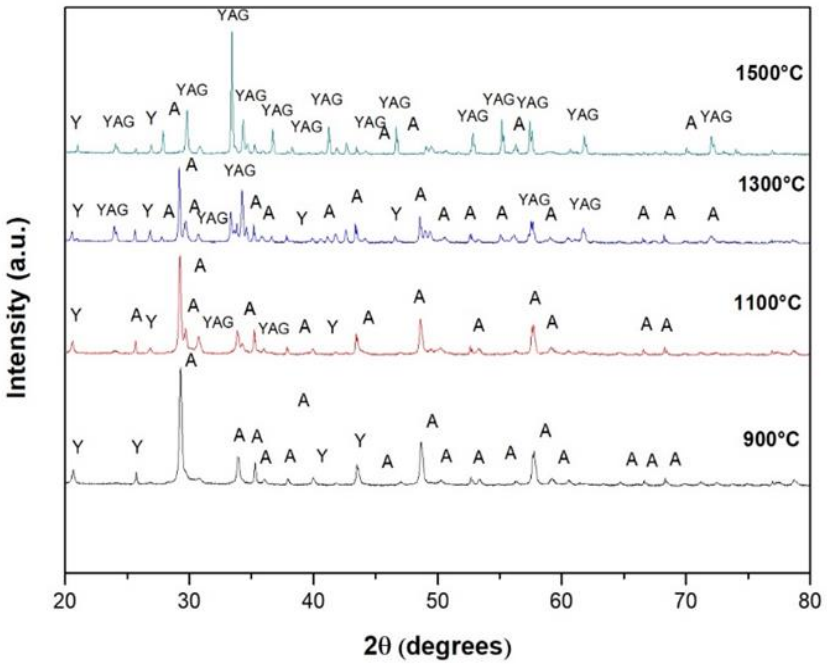

Figure 3. Diffraction patterns of the powder mixture Y_2O_3 + Al_2O_3 subjected to interrupted tests at different temperatures to determine the formation temperature of yttrium-aluminum garnet ($Y_3Al_5O_{12}$).

Diffractions in resulting spectrum at 1,500 °C correspond to Nd-YAG in agreements with JCPDS 79-1892. The unit cell of Nd-YAG was calculated by the least square method using all reflections of Nd-YAG in spectrum at 1,500 °C of figure 3. The calculated result reveals that the crystals have body-centered cubic crystalline structure with space group Ia3d. The lattice parameter for YAG with different addition of Nd are presented in Table 1.

Table 1. Lattice parameter of the Nd:YAG crystalline cubic structure, as a function of Nd in the compo.

Nd atomic %	Lattice parameter
0	11.9604
0.25	11.9712
0.5	11.9771
1	11.9814

The lattice parameter values increase with increasing neodymium in the $Y_3Al_5O_{12}$ compound due to the slightly larger atomic radius of neodymium (1.82 Å) with respect to yttrium (1.80 Å). However, these values are similar to those reported in literature [7, 16-17].

3.4 Fourier-transform infrared spectroscopy

Figure 4 shows the absorbance spectrum obtained by Fourier-transform infrared spectroscopy of the sample sintered at 1,500°C. This spectrum shows two peaks at 591 and 1034 cm^{-1} which have been associated with the Al-O functional group of alumina. On the other hand, at wavenumbers of 1411 and 1510 cm^{-1}, two other peaks are observed, corresponding to the Y-O functional group matching the yttria. Finally, at 3300 cm^{-1} one more peak was observed, which was associated with the H-O bond corresponding to

Preprints (www.preprints.org) | NOT PEER-REVIEWED | Posted: 17 May 2023 doi:10.20944/preprints202305.1250.v1

water. The presence of this chemical bond is due to the absorption of water by the sample after it was sintered. From this spectrum, it can be confirmed that the functional groups composing the mixture are those corresponding to the elements of the compound $Y_3Al_5O_{12}$.

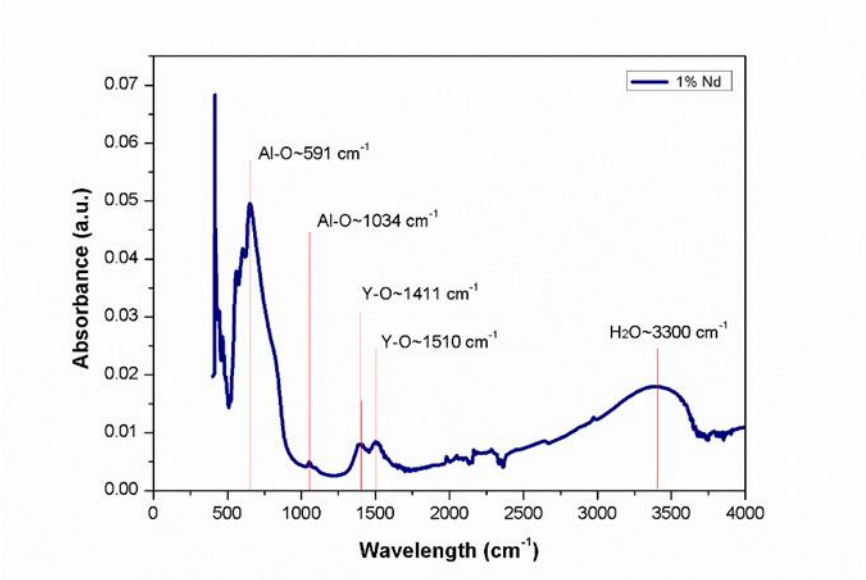

Figure 4. FTIR spectrum obtained from the sample sintered at 1,500°C with addition of 1 at. %Nd.

3.5 Absorption Spectrum

Absorption studies were performed for the samples with additions of Nd in atomic percentages from 0.25%, 0.5% and 1%. Figure 5 shows the comparative absorption spectra for each of the samples. Predominant absorption bands can be better observed from the 1% Nd sample at around 750 and 810 nm, corresponding to transitions from the $^4I_{9/2}$ ground level to $^4F_{7/2}$:$^4S_{3/2}$ and $^4F_{5/2}$:$^4H_{9/2}$ levels, respectively. In addition, peaks at 520, 590 and 880 nm are also present. It can be seen that the bandwidth and the peak shape are the same for the samples with neodymium content, however, as the concentration increases, the peak absorbance is greater.

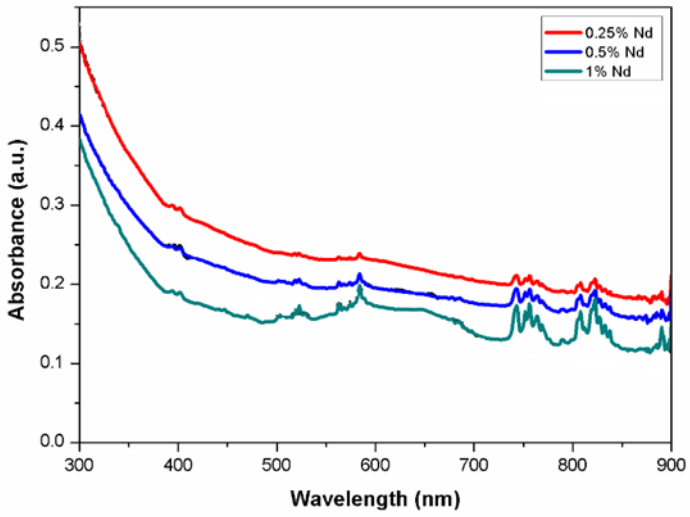

Figure 5. Absorption spectra of Nd in YAG.

3.6 Emission Spectrum

Preprints (www.preprints.org) | NOT PEER-REVIEWED | Posted: 17 May 2023 doi:10.20944/preprints202305.1250.v1

Emission studies were carried out at wavelengths from 930 to 1370 nm for the three samples doped with Nd. Figure 6 shows the comparative emission spectra for each of the samples. As can be seen, the peak intensity increases as neodymium concentration increases. Still, the shape of the peaks and the bandwidth are maintained in all cases, which is important in laser emission applications. The emission spectra are presented in the three predominant regions due to radiative decay from the $^4F_{3/2}$ state to the $^4I_{9/2}$, $^4I_{11/2}$ and $^4I_{13/2}$ states that can be seen in the figure. The energy levels of Nd:YAG are determined by the neodymium (Nd) ions in the YAG, the predominant radiative transition at 1064 nm occurs between the upper stark level of the $^4F_{3/2}$ state and one of the $^4I_{11/2}$ states. The synthesized materials could have potential application in the development of a laser that emits in the near infrared region.

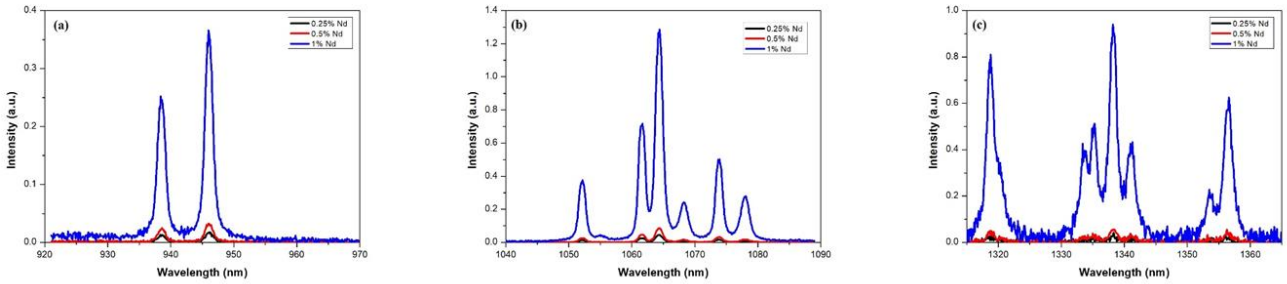

Figure 6. Emission spectra of Nd:YAG for (a) transition $^4F_{3/2} \rightarrow {}^4I_{9/2}$, (b) transition $^4F_{3/2} \rightarrow {}^4I_{11/2}$ and (c) transition $^4F_{3/2} \rightarrow {}^4I_{13/2}$.

3.7 Microstructure

The microstructures of synthesized Nd:YAG, taken from the optical microscope are shown in Figure 7. In general, the microstructure is very fine made up of irregular grains of different sizes and morphologies (angular, rounded, etc.). Due to the fine microstructure, the porosity of the samples cannot be distinguished. Apparently, finer particles are obtained for intermediate Nd contents (0.25 at. % and 0.5 at. %). However, the sample with 0.5 at. % Nd is cracked. According to density measurements, the higher the amount of Nd in the garnet, the lower the bulk density, a situation difficult to observe in these images. However, the very fine size present in these composites due to the type of processing carried out to manufacture them positively influences the optical properties of the composites, as already observed above. This suggests that if the processing conditions of these composites can be better controlled to obtain denser bodies, the optical properties will be further improved.

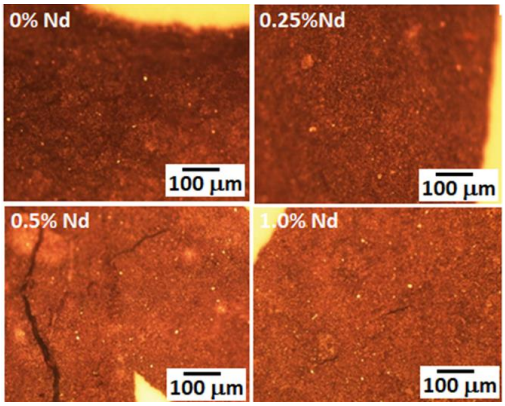

Figure 7. Microstructures of different synthesized Nd:YAG, taken from the optical microscope.

5. Conclusions

Preprints (www.preprints.org) | NOT PEER-REVIEWED | Posted: 17 May 2023 doi:10.20944/preprints202305.1250.v1

Through intense mixing of the ceramics Al_2O_3 and Y_2O_3 in a high energy mill and subsequent heat treatment at elevated temperature to induce solid state chemical reactions between the two initial components, the synthesis of the compound $Y_3Al_5O_{12}$ doped with different percentages of neodymium was feasible. From the characterizations performed on the products obtained, the following results were obtained: X-ray diffraction patterns indicate that the formation of the $Y_3Al_5O_{12}$ compound by solid-state reaction starts at approximately 1100°C and is completed at 1500°C; likewise, the newly formed compound has a cubic crystalline structure. The spectra obtained by Fourier transform infrared spectroscopy show the presence of the 2 functional groups (Al-O and Y-O) of the $Y_3Al_5O_{12}$ compound. The analysis by optical absorption and emission spectroscopy indicates wavelength bands in agreement with the electronic structure of Nd ions in YAG. The microstructure of the manufactured composite is very fine, presenting equiaxial grains with sizes of less than 1 micron. This explains the good optical characteristics of the manufactured compound. The results are promising for the development of a light source based on a ceramic material obtained by the solid-state reaction method.

Author Contributions: Conceptualization, GVVG, ERR and CACA; methodology, OAER, JACR and JLH; validation, JACR, JLH and WJPR.; formal analysis, OAER, GVVG, ERR and CACA; investigation, OAER, JACR and JLH; resources, GVVG, JACR, JLH, CACA, WJPR and ERR; data curation, OAER, GVVG, JACR and JLH and JARG; writing—original draft preparation, OAER, GVVG, CACA and ERR; writing—review and editing, GVVG and CACA; visualization, GVVG, CACA and ERR; supervision, GVVG, CACA and ERR; project administration, ERR; All authors have read and agreed to the published version of the manuscript.

Funding: This research work did not receive any type of support for its realization.

Informed Consent Statement: Not applicable.

Data Availability Statement: Not applicable.

Acknowledgments: OAER thanks the national council of science and technology for the scholarship granted for the completion of her master's studies.

Conflicts of Interest: The authors declare no conflict of interest.

References

1. S. Nakai, K. Mima, Laser driven inertial fusion energy: present and prospective, Rep. Prog. Phys., **2004**, 67 321-325. doi:10.1088/0034-4885/67/3/R04.
2. A. Ikesue, Y. Lin Aung, T. Taira, T. Kamimura, K. Yoshida, G. L. Messing, Progress in Ceramic Lasers, Annu. Rev. Mater. Res., **2006**, 36 [1] 397-429. doi.org/10.1146/annurev.matsci.36.011205.152926.
3. A. Ikesue, Y. L. Aung, Ceramic laser materials, Nat. Photon, **2008**, 2 721–727. doi.org/10.1038/nphoton.2008.243.
4. L. Chang-qing, Z. Hong-bo, Z. Ming-fu, H. Jie-cai, M. Song-he, Fabrication of transparent YAG ceramics by traditional solid-state-reaction method, T. Nonferr. Metal. Soc. of China, **2007**, 17 [1] 148-153. doi: 10.1016/S1003-6326(07)60064-8.
5. P. Jongnam, J. Joo, S. Gu Kwon, Y. Jang, T. Hyeon, Synthesis of Monodisperse Spherical Nanocrystals, Angewandte International Edition Chemie, **2007**. doi.org/10.1002/anie.200603148.
6. R. Boulesteix, A. Maître, J. F. Baumard, C. Sallé, Y. Rabinovitch, Mechanism of the liquid-phase sintering for Nd:YAG ceramics, Opt. Mater., **2009**, 31 [5] 711-715. doi:10.1016/j.optmat.2008.04.005.
7. S. Kostić, Z. Ž. Lazarević, V. Radojević, A. Milutinović, M. Romčević, N. Ž. Romčević, A. Valčićb, Study of structural and optical properties of YAG and Nd:YAG single crystals, Mater. Res. Bull., **2015**, 63 80-87. doi.org/10.1016/j.materresbull.2014.11.033.
8. L. Chrétien, R. Boulesteix, A. Maître, C. Sallé, Y. Reignoux, Post-sintering treatment of neodymium-doped yttrium aluminum garnet (Nd:YAG) transparent ceramics, Opt. Mater. Express, **2014**, 4 [10] 2166-2173. doi: 10.1364/ome.4.002166.
9. Y. Su, D. M. Xin, X. Chen, W. Xing, Effect of CAD-CAM ceramic materials on the color match of veneer restorations, J. Prosthet. Dent., **2021**, 126 [2] 255.e1-255.e7. doi:10.1016/j.prosdent.2021.04.029.
10. M. Rubat du Merac, Transparent Ceramics: Materials, Processing, Properties and Applications, Editor: Michael Pomeroy, Encyclopedia of Materials: Technical Ceramics and Glasses, Elsevier, Ámsterdam, **2021**.
11. A. Vorona, A. Balabanov, M. Dobrotvorska, R. Yavetskiy, O. Kryzhanovska, L. Kravchenko, S. Parkhomenko, P. Mateychenko, V. Baumer, I. Matolínová, Effect of MgO doping on the structure and optical properties of YAG transparent ceramics, J. Eur. Ceram. Soc., 2020, 40 [3] 861-866. doi.org/10.1016/j.jeurceramsoc.2019.10.048Get.
12. W. Jia, C. Su, H. Zhang, X. Zou, G. Ren, Q. Wei, M. Zhao, C. Ma., Quantitative relationship between microstructure and mechanical properties in Nd: YAG transparent ceramics, Ceram. Int., **2021**, 47 [9] 12144-12152. doi.org/10.1016/j.ceramint.2021.01.061.

Preprints (www.preprints.org) | NOT PEER-REVIEWED | Posted: 17 May 2023 doi:10.20944/preprints202305.1250.v1

13. N. Jiang, C. Ouynag, Y. Liu, W. Li, Y. Fu, T. Xie, Q. Liu, Y. Pan, J. Li, Effect of air annealing on the optical properties and laser performance of Yb:YAG transparent ceramics, Opt. Mater., 95, **2019**. doi:10.1016/j.optmat.2019.109203.
14. D.Yu. Kosyanov, A. A. Vornovskikh, A. M. Zakharenko, E. A. Gridasova, R. P. Yavetskiy, M. V. Dobrotvorskaya, A. V. Tolmachev, O. O. Shichalin, E. K. Papynov, A. Y. Ustinov, V. G. Kuryavyi, A. A. Leonov, S. A. Tikhonov, Influence of sintering parameters on transparency of reactive SPSed Nd^{3+}:YAG ceramics, Opt. Mater., **2021**, 112. [doi:10.1016/j.optmat.2020.110760].
15. ASTM C20-00, Standard test methods for apparent porosity, water absorption, apparent specific gravity, and bulk density of burned refractory brick and shapes by boiling water **2010**.
16. A. Golubovic, S. Nikolić, R. Gajić, S. Đurić, A. Valčić, The growth of Nd: YAG single crystals, J. Serb. Chem. Soc., **2002**, 67 [4] 291–300. doi.org/10.2298/JSC0204291G.
17. A. Golubovic, S. Nikolic, R. Gajić, Z. Dohčević-Mitrović, A. Valčić, Growth and IR Spectra of YAG and Nd:YAG Single Crystals, J. Metal., 2004, 10 [4] 363-370.